**Production of affinity-purified antibodies to phospho-Ser1987 mouse ATM**
The anti-phospho mouse *ATM*-Ser1987 rabbit polyclonal antibody (PickCell Laboratories BV, Amsterdam, The Netherlands) was raised against a peptide KRSPTFEEGSpQGTTI, containing amino acids surrounding Ser1987 from mouse *ATM*. Rabbits were injected and boosted 3 times. The antiserum was affinity-purified, and specificity of antibodies was determined by immunoblotting (1:1000 dilution, Fig. S14).

**Electron microscopy**
Animals were anesthetized using *isoflurane and tissue perfusion was performed* using a perfusion-wash solution followed by a perfusion-fix solution (Electron Microscopy Science Company). Thymuses were harvested and analyzed using a JEOL Electron Microscope.

**Reverse transcription-real time PCR and siRNA treatment**
For siRNA treatment against human *Beclin-1,* human fibroblasts were transfected with On-TARGETplus SMART pool siRNAs (Thermo Scientific, # L-010552-00-0020) at 100 nM final concentration using Dharmafect 1 transfection reagent (Thermo Scientific). 24 hr later, cells were treated with 50 μM CCCP (4 hr) followed by total RNA isolation. Total RNA was isolated from human fibroblasts or viable thymocytes using the RNeasy kit (Qiagen) as indicated by the company. Reverse transcription was performed in 1–2 μg RNA using the First Strand cDNA Synthesis kit (GE Healthcare). Absolute quantification of mRNA was done by real time PCR using the primers sets shown in Table S1.

**Mitochondrial DNA content:**
Total cellular DNA was extracted using the DNeasy kit (Qiagen). The amount of mitochondrial DNA/nuclear DNA was determined by quantitative real-time PCR using primers shown in Table S1. Relative *ND1* (or *ND2*) copy number is calculated based on the threshold cycle (Ct) as $2^{-\Delta(\Delta CT)}$, where $\Delta Ct = Ct_{ND1\ (or\ ND2)} - C_{18S}$, and $\Delta(\Delta Ct) = \Delta Ct_{sample} - \Delta Ct_{control}$.

**Superoxide measurements**
5mM MitoSOX reagent stock solution (Molecular Probes) was prepared by dissolving one vial of MitoSOX in 13 μL DMSO and the stock solution was added to 13 mL DMEM to a final concentration of 5 μM. Cells were centrifuged and resuspended into 500 μL DMEM containing MitoSOX. Cells were incubated at 37$^{o}$C for 10 min and analyzed by flow cytometry.

**Statistical analyses**
All statistical tests were performed as indicated in figure legends using the GraphPad Prism 5 program.

**Table S1. Primers used for assessment of mitochondrial DNA/nuclear DNA or reverse transcription-real time PCR analyses**

| Gene | Forward primer | Reverse primer |
|---|---|---|
| ***human NADH dehydrogenase subunit 1 (ND1)*** | cccgccacatctaccatca | gaagagcgatggtgagagctaag |
| **mouse *NADH dehydrogenase subunit 2 (ND2)*** | cccattccacttctgattacc | atgatagtagagttgagtagcg |
| **human/mouse nuclear *18S* rRNA** | tagagggacaagtggcgttc | cgctgagccagtcagtgt |
| **human *Nrf2*** | gcgacggaaagagtatgac | gttggcagatccactggttt |
| **mouse *Nrf2*** | ctcgctggaaaaagaagtg | ccgtccaggagttcagagg |
| **mouse *Nqo1*** | agctggaagctgcagacctg | cctttcagaatggctggca |
| **mouse *PRC*** | tgccttgcagttactcatgc | ctgacttgcactggcaggta |
| **mouse *PGC1-β*** | tgcagctaagagaccatgagatccgt | gcttctttagttcccgagagctcatgtc |
| **mouse *Nrf1*** | tggtccagagagtgcttgtg | ttcctgggaagggagaagat |
| **mouse *SOD2*** | gcggtcgtgtaaacctcat | ccagagcctcgtggtacttc |

**Figure S1. Abnormal mitochondrial function in ATM-deficient thymocytes**
(A) Transmission electron microscopy (TEM) of whole thymus tissue of an *ATM*$^{-/-}$ mouse displaying a massive increase in mitochondrial number. Of 5 *ATM*$^{-/-}$ mice analyzed by TEM, one showed a very drastic increase in the number of both normal and abnormal (asterisks) mitochondria within the thymus. (B) *ATM-deficient thymocytes* display an increase in the number of thymic cells with high membrane potential. Tetramethylrhodamine (TMRE) staining was performed in freshly isolated viable thymocytes of wild type and *ATM*$^{-/-}$ mice. Shown in a representative histogram of each genotype. Arrowheads point cell populations with high membrane potential. At least 10,000 cells were analyzed per sample. Graph illustrates the average percentage of cells displaying high membrane potential. (n = 2 per genotype).

**Figure S2. Culture and/or immortalization of cells affect mitochondrial metabolism and autophagy signaling, and alter the impact of ATM deficiency**
(A–C) Mitochondrial abnormalities in immortalized human fibroblasts or lymphoblasts, and mouse embryonic fibroblasts (MEFs), lacking *ATM*. hTERT-immortalized human fibroblasts (A) or EBV-immortalized human A-T lymphoblasts (B) were analyzed for mitochondrial DNA content by real-time PCR analysis of mitochondrial/nuclear ratio (*ND1*/*18S* rRNA). Relative mitochondrial DNA content assessed by real-time PCR analysis of mitochondrial/nuclear ratio (*ND1*/*18S* rRNA) is shown. (C) Immortalized MEFs lacking both *ATM* and *Arf* display similar mitochondrial DNA content as immortalized *Arf*-deficient MEFs. Total cellular DNA was isolated from the immortalized MEFs of passage 9 (P9) and the relative mitochondrial DNA content was analyzed by real-time PCR of mitochondrial/nuclear ratio (*ND2*/*18S* rRNA). (D) *Ex vivo* culture alters mitochondrial homeostasis. The mitochondrial DNA content of MEFs isolated from the indicated mice was analyzed with cellular passage (P0-P4) as in A–C using primers against *ND2* (mitochondrial) and *18S* rRNA (nuclear) genes.

**Figure S3. Parkin localizes to mitochondria in immortalized human A-T fibroblasts**
hTERT-immortalized normal or A-T human fibroblasts were transfected with a plasmid expressing YFP-Parkin for 24 hours and then stained against the mitochondrial marker TOM-20. YFP-Parkin immunofluorescence (green) is diffusely distributed in normal cells (top panel) while it has a more punctate distribution that overlaps with TOM-20 staining (red) in A-T cells. Nuclei are visualized with DAPI (blue). Magnification ×400.

**Figure S4. *Ex vivo* culture alter autophagic responses**
Immunoblot analyses of autophagic signaling molecules (p62 and LC3), and the oxidative damage sensor DJ-I in MEFs with passage *ex vivo* (P0-P4). Actin served as a loading control. *ATM*-deficient fibroblasts show elevated autophagic responses at early passage (P0) as compared to control fibroblast of the same passage.

**Figure S5. Analyses of ATM and Beclin-1 in thymocytes demonstrate that allelic loss of Beclin-1 results in decreased levels of Beclin-1 protein**
20 μg of total protein from thymocytes of the indicated mice were analyzed by immunoblotting against total ATM, Beclin-1, and Actin (loading control).

**Figure S6. ATM deficiency augments basal LC3 punctae in early passage MEFs and allelic loss of Beclin-1 rescues this phenotype**
Immunofluorescence analyses of endogenous LC3 in P2 and P4 MEFs are shown. As control for staining LC3 punctae, wild-type MEFs were transiently treated with 50 μM Chloroquine (CQ) for three hr. LC3 staining is visualized in green. DAPI staining (blue) was used to mark nuclei.

**Figure S7. Allelic loss of Beclin-1 partially rescued the increased apoptotic index observed in ATM-deficient thymocytes**
(A) *Beclin-1* heterozygosity augments the numbers of *ATM*-deficient thymocytes. Whole thymus was isolated from mice of the indicated genotypes and single cell suspensions were prepared. Total cell number was determined using Vi-Cell XR analyzer (Beckman). (B) Allelic loss of *Beclin-1* rescues cell death manifest in $ATM^{-/-}$ thymocytes. The percent of viable thymocytes was determined in freshly isolated thymocytes of 5–8 week old mice by propidium iodide exclusion followed by flow cytometry (** $P \leq 0.001$; ***, $P \leq 0.001$; $n \geq 3$ per group).

**Figure S8. Beclin-1 heterozygosity reduces the elevated basal levels of the mitochondrial Tom20 observed in ATM-deficient cells**
Immunofluorescence against the mitochondrial protein Tom20 (red) was performed in paraffin-embedded thymic tissues from of 6–8 week old mice of desired genotypes. Blue stains nuclei. Magnification ×400 ($n \geq 2$ per genotype).

**Figure S9. Beclin-1 heterozygosity reduces the mitochondrial mass phenotype manifest in ATM-deficient thymocytes**
Freshly isolated thymic cells were stained with 200 nM Mitotracker Green (MTG) probe (A) or with 5 nM Nonyl Acridine Orange (NAO) dye (B). Graphs illustrate the averaged mean intensity of MTG or NAO for each genotype. *P* values were obtained by the Student *t*-Test ($n \geq 2$ per genotype).

**Figure S10. Immortalized A-T fibroblasts show a significant increase in oxygen consumption rate (OCR)**
OCR as a function of time (minutes) was assessed in an equal number of viable control and A-T fibroblasts. Two runs per sample are shown.

**Figure S11. Genes involved in oxidative stress responses are induced in ATM-null cells and this response is reversed by Beclin-1 heterozygosity**
(A–B) Total cellular RNA was isolated from viable thymocytes of the indicated genotypes and the mRNA levels of genes involved in antioxidant defense (*Nrf2, Nqo1*) were measured by reverse transcription real-time PCR analyses. mRNA levels were normalized using *Actin* transcripts as an internal control. Each dot, triangle, and square represents a single animal analyzed (*, $P < 0.01$; **, $P < 0.001$). (C) *Beclin*-1 knockdown reverses the increase in *Nrf2* mRNA levels observed in immortalized A-T fibroblasts. Immortalized human fibroblasts (wild type or ATM [A-T]–deficient) were transfected with 100 nM siRNA pools against human *Beclin-1* for 24 hr followed by treatment with DMSO or 50 μM CCCP for 4 hr. Total RNA was harvested and the *Nrf2* transcripts were analyzed by reverse transcription-real time PCR using *Actin* mRNA as internal control. Note that *Beclin-1* knockdown also blunts the rise in *Nrf2* mRNA levels caused by CCCP treatment.

**Figure S12. Allelic loss of Beclin-1 does not alter mitochondrial mass content of Eμ-Myc B cells**
$B220^+$ bone marrow B cells were harvested from the indicated mice and mitochondrial mass was determined by staining cells with Mitotracker CMRos (Molecular probes) followed by flow cytometry. The averaged Mitotracker fluorescence intensity (MFI) is shown for each cohort. *P* values were obtained by the Student *t*-Test ($n \geq 3$ per genotype)**.**

**Figure S13. Proposed model of tumor development in the absence of ATM**
Loss of *ATM* in T cells results in an increased number of aberrant mitochondria, possibly due to inefficiency of these cells to engage mitophagy, and to defects in Complex I activity. Abnormal mitochondria leads to an increase in mitochondrial ROS, which in turn may function synergistically with alterations in DNA damage signaling to facilitate T cell tumorigenesis in *ATM*-null mice and in patients with A-T. The enhanced autophagy response in the absence of *ATM* is likely triggered by the mitochondrial ROS generated in these cells and by abnormal, damaged mitochondria. The rescue of mitochondrial dysfunction and marked delay in tumor onset in *ATM*-null mice associated with allelic loss of *Beclin-1* may relate to a role of Beclin-1 in mitochondrial homeostasis independent of its autophagic function. The finding that a fraction of ATM localizes at mitochondria and becomes active after mitochondrial damage suggests that ATM plays a direct role within this organelle to protect normal mitochondrial function and/or promote mitophagy.

**Figure S14. Characterization of the mouse phospho-Ser1987 ATM antibody**
Human foreskin fibroblasts (HFF) or MEFs, including $ATM^{-/-}$ MEFs, were irradiated using 5 Gy, allowed to recover for 1 hour, and were analyzed by SDS-PAGE. Immunoblotting was performed using antibodies against total human/mouse ATM (MAT-3), phospho-S1987 ATM (mouse), phospho-S1981 ATM (human), human/mouse phospho-S957 SMC1, and Actin.

# Figure S1

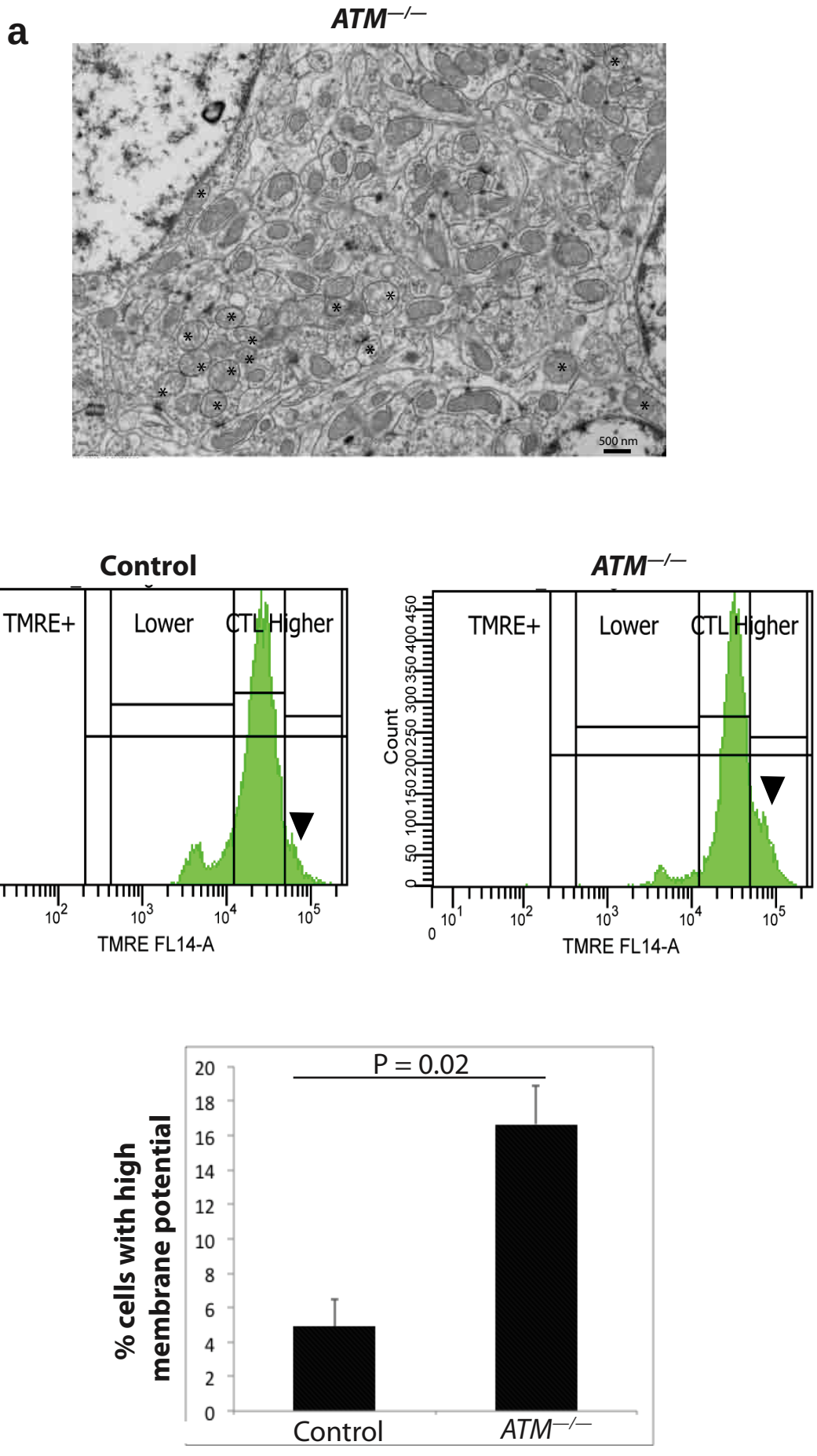
a
ATM−/−
500 nm
b
Control
ATM−/−
TMRE+
Lower
CTL Higher
Count
TMRE FL14-A
P = 0.02
% cells with high membrane potential
Control
ATM−/−

# Figure S2

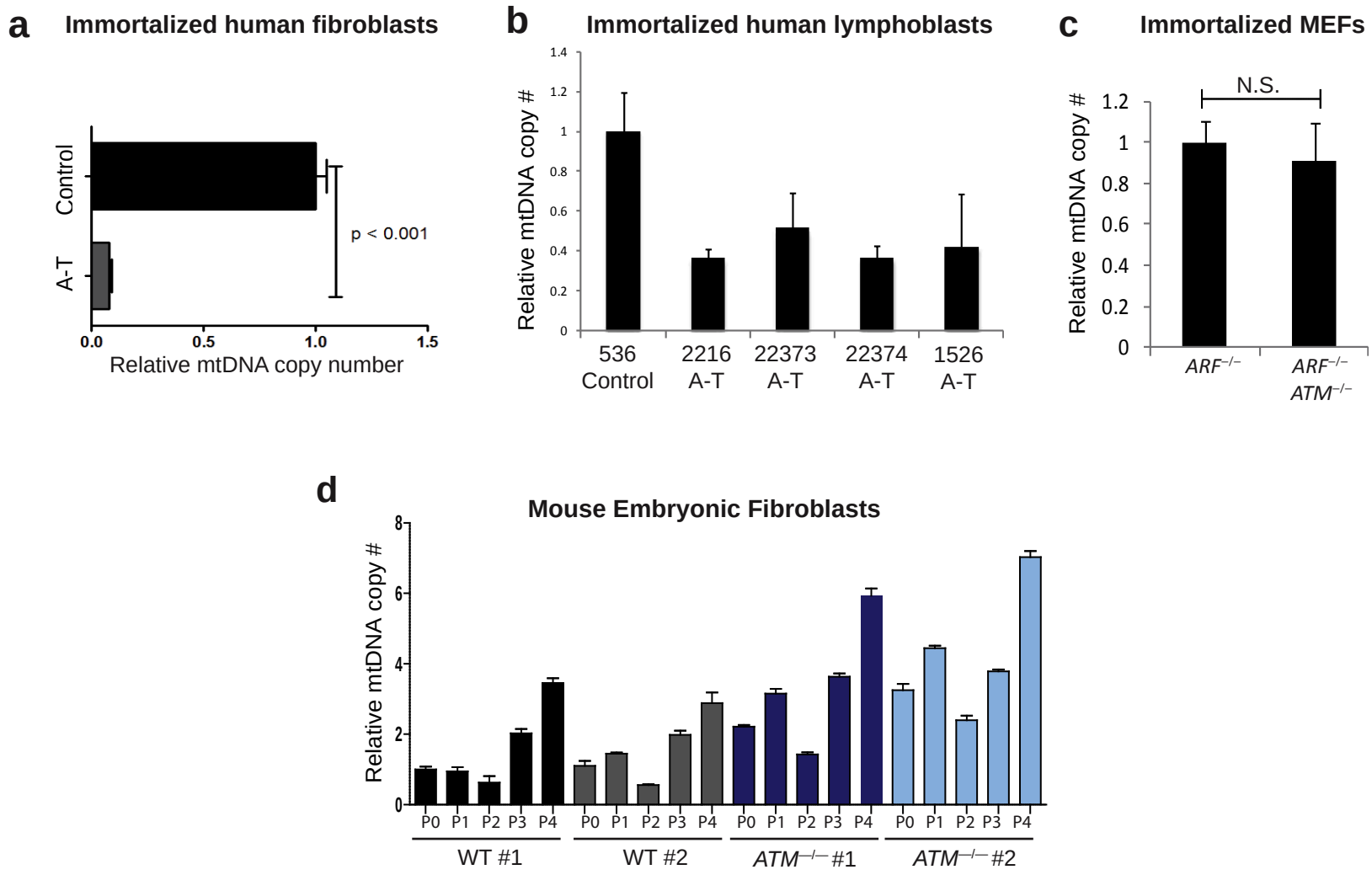
a
Immortalized human fibroblasts
Control
A-T
p < 0.001
0.0
0.5
1.0
1.5
Relative mtDNA copy number
b
Immortalized human lymphoblasts
Relative mtDNA copy #
1.4
1.2
1
0.8
0.6
0.4
0.2
0
536
Control
2216
A-T
22373
A-T
22374
A-T
1526
A-T
c
Immortalized MEFs
N.S.
Relative mtDNA copy #
1.2
1
0.8
0.6
0.4
0.2
0
ARF−/−
ARF−/−
ATM−/−
d
Mouse Embryonic Fibroblasts
Relative mtDNA copy #
8
6
4
2
0
P0 P1 P2 P3 P4
P0 P1 P2 P3 P4
P0 P1 P2 P3 P4
P0 P1 P2 P3 P4
WT #1
WT #2
ATM−/− #1
ATM−/− #2

# Figure S3

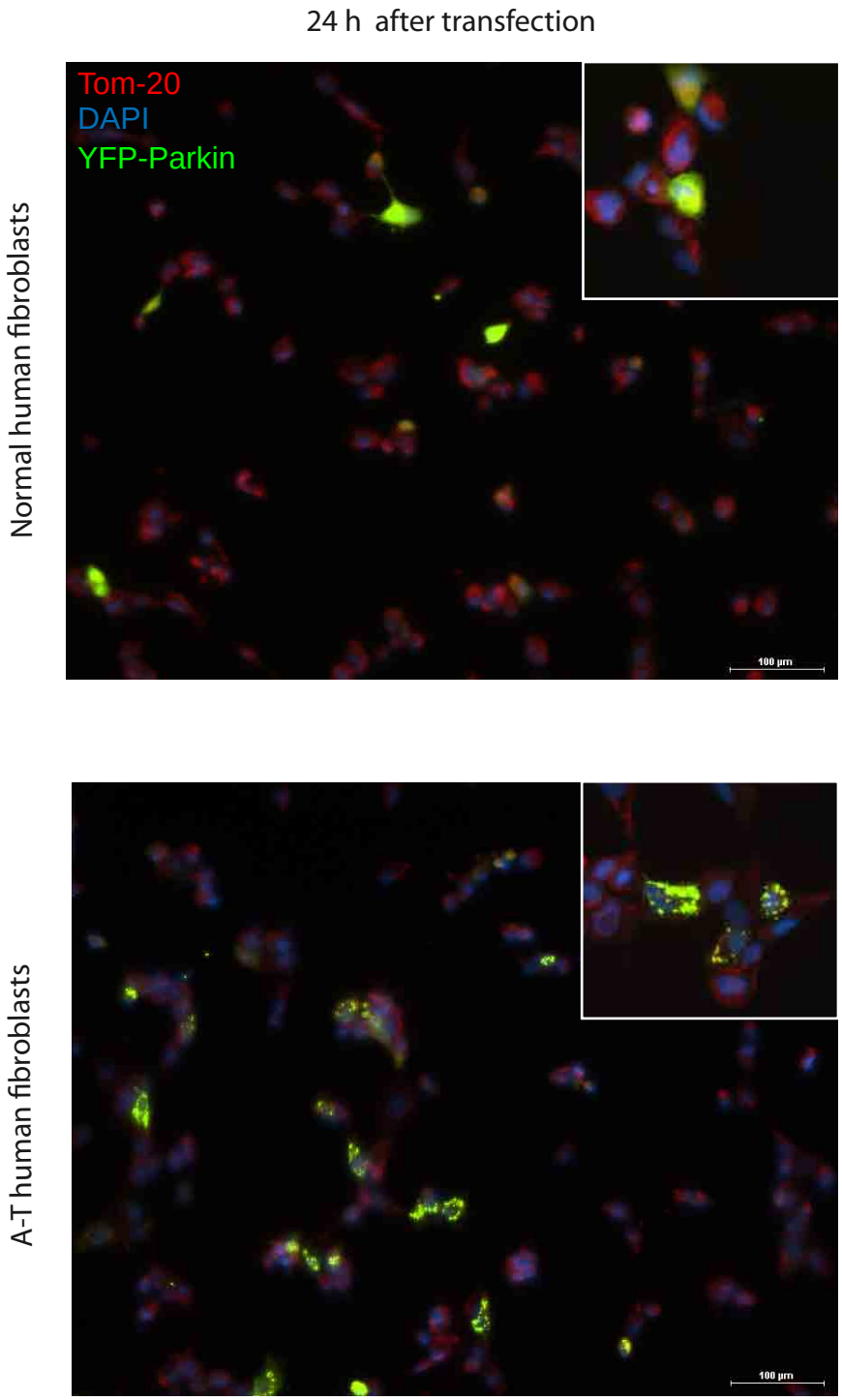
24 h after transfection
Tom-20
DAPI
YFP-Parkin
Normal human fibroblasts
A-T human fibroblasts
100 µm
100 µm

# Figure S4

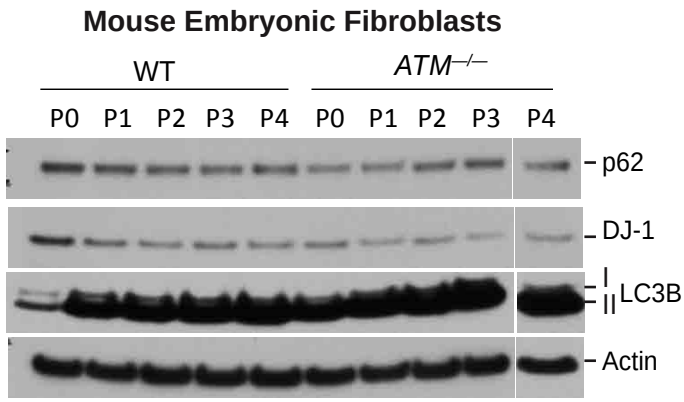
Mouse Embryonic Fibroblasts
WT
ATM−/−
P0 P1 P2 P3 P4 P0 P1 P2 P3 P4
p62
DJ-1
I
II
LC3B
Actin

# Figure S5

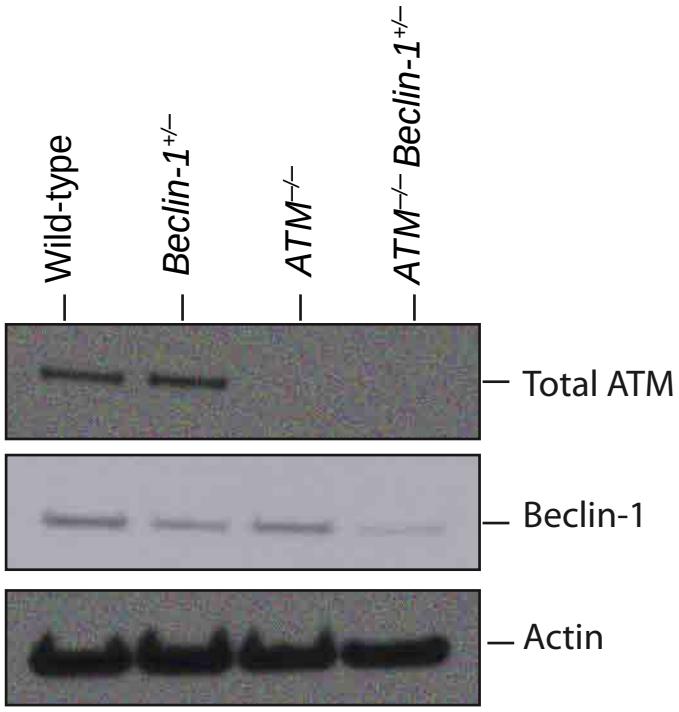

**Figure S6**

Mouse Embryonic Fibroblasts

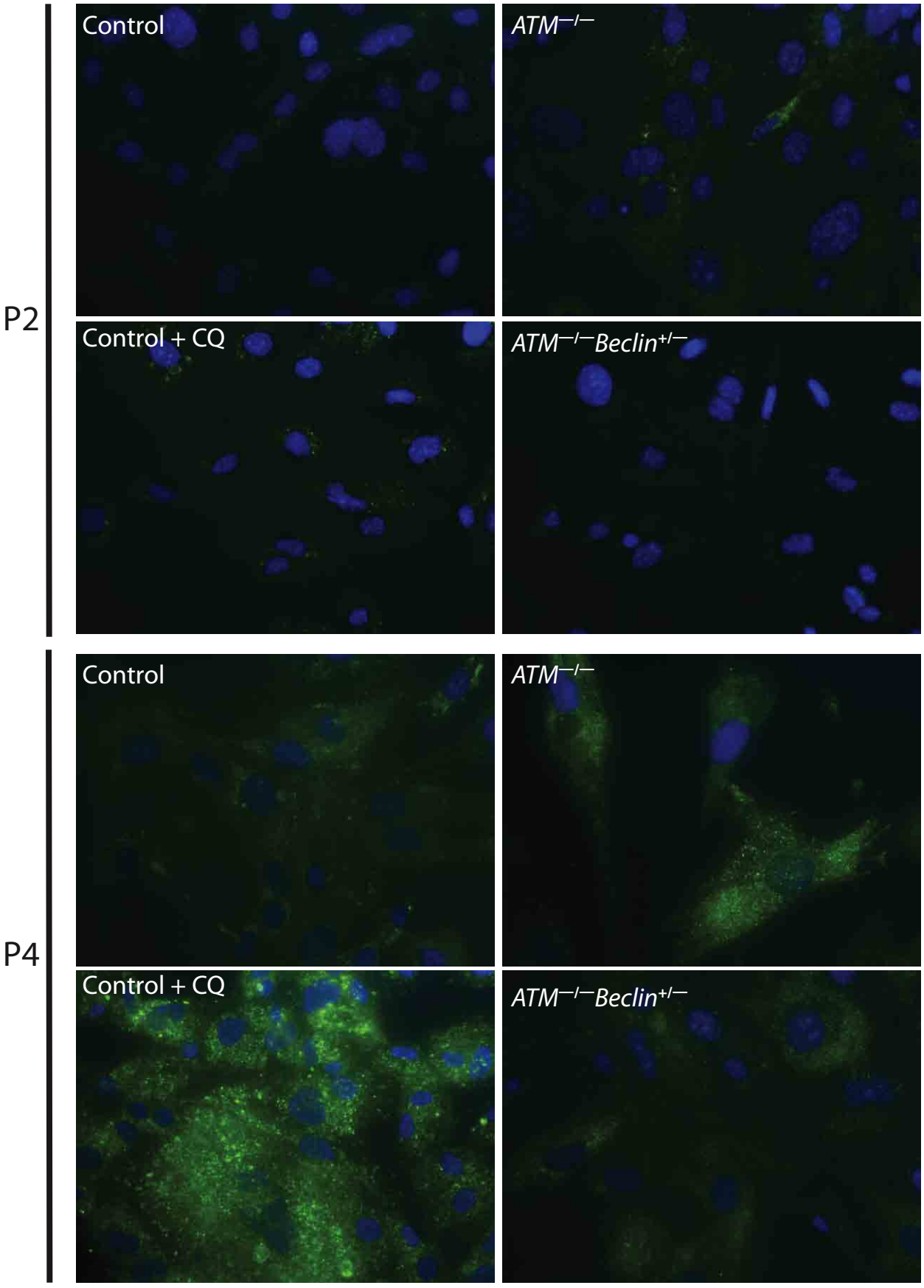

**Figure S7**

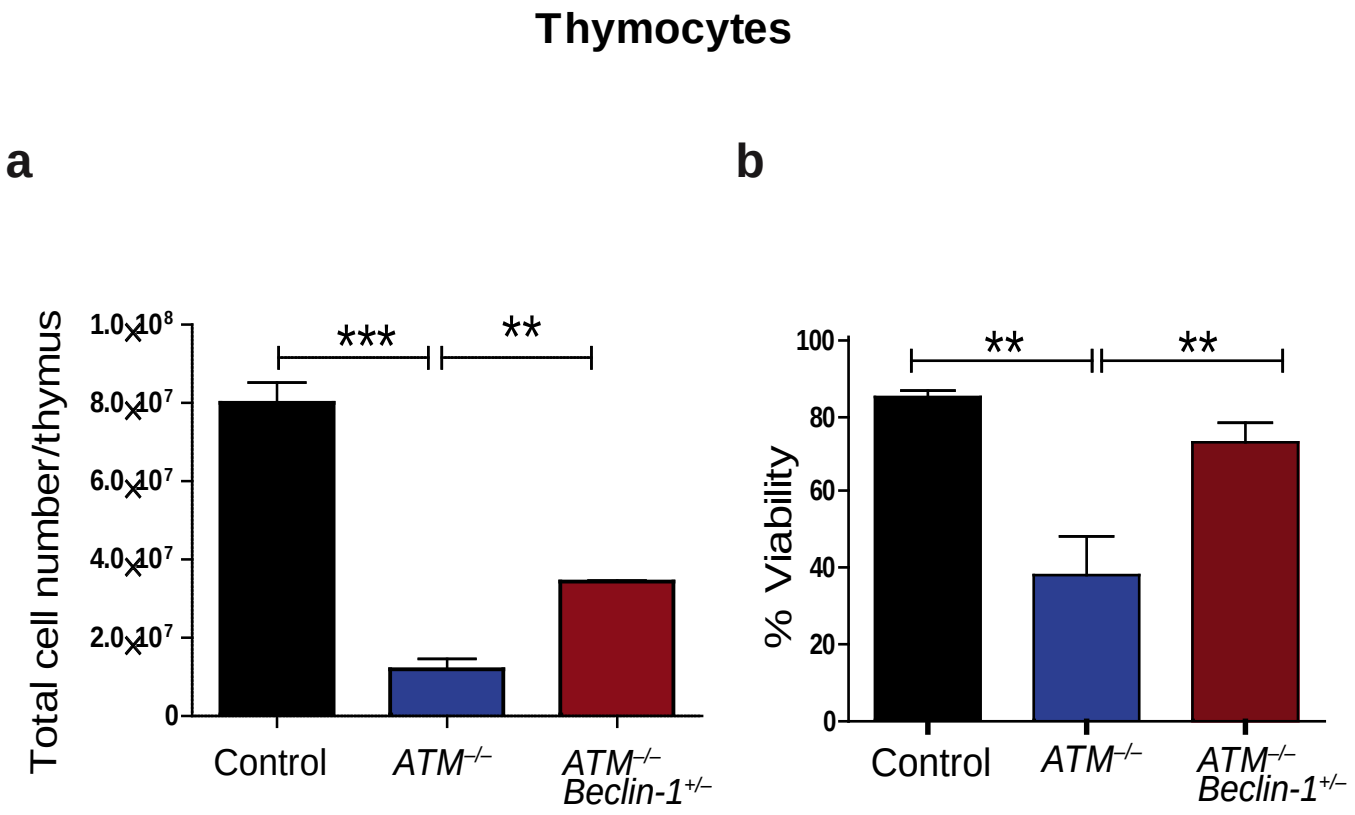
Thymocytes
a
b
Total cell number/thymus
1.0x10^8
8.0x10^7
6.0x10^7
4.0x10^7
2.0x10^7
0
***
**
Control
ATM−/−
ATM−/− Beclin-1+/−
% Viability
100
80
60
40
20
0
**
**
Control
ATM−/−
ATM−/− Beclin-1+/−

# Figure S8

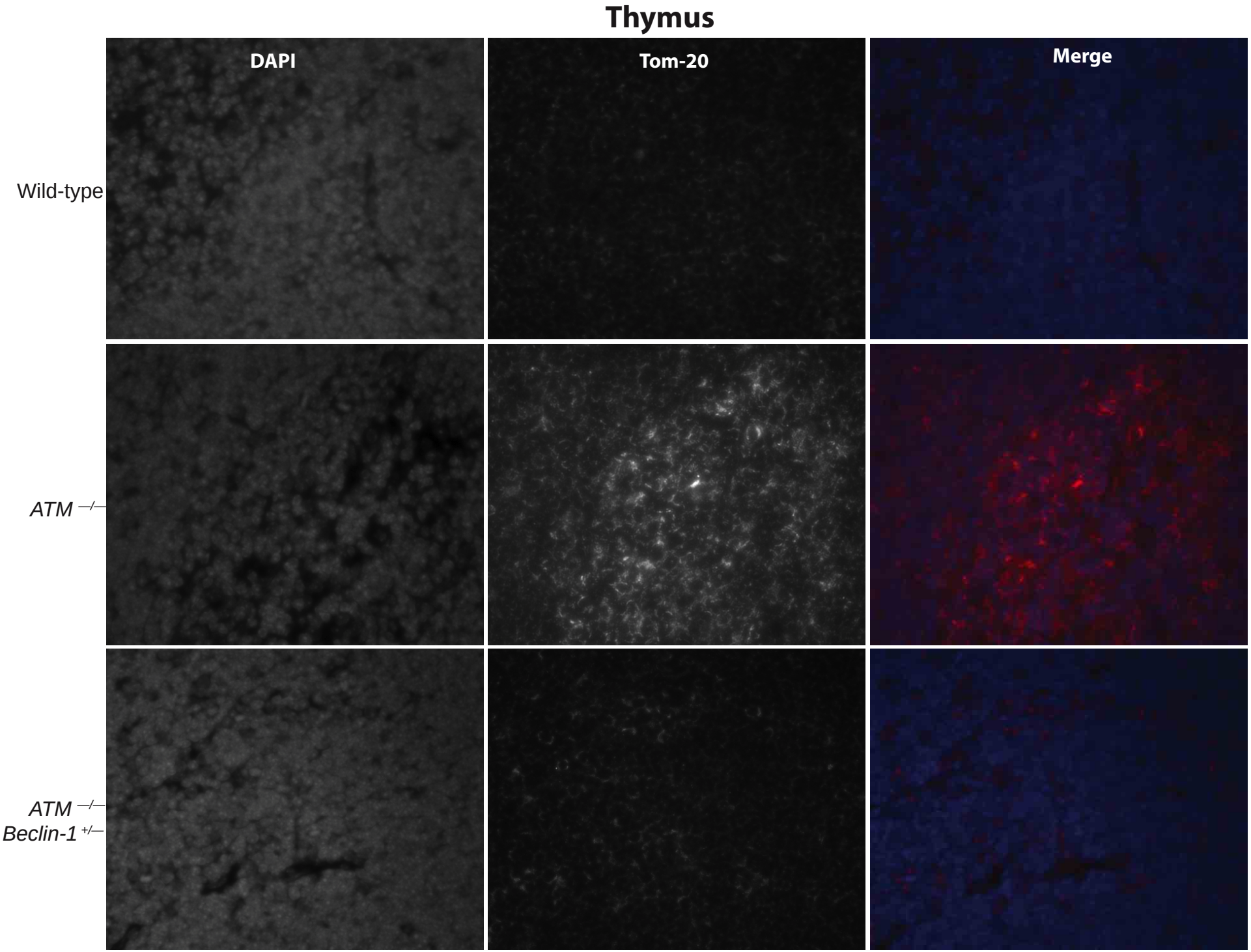

# Figure S9

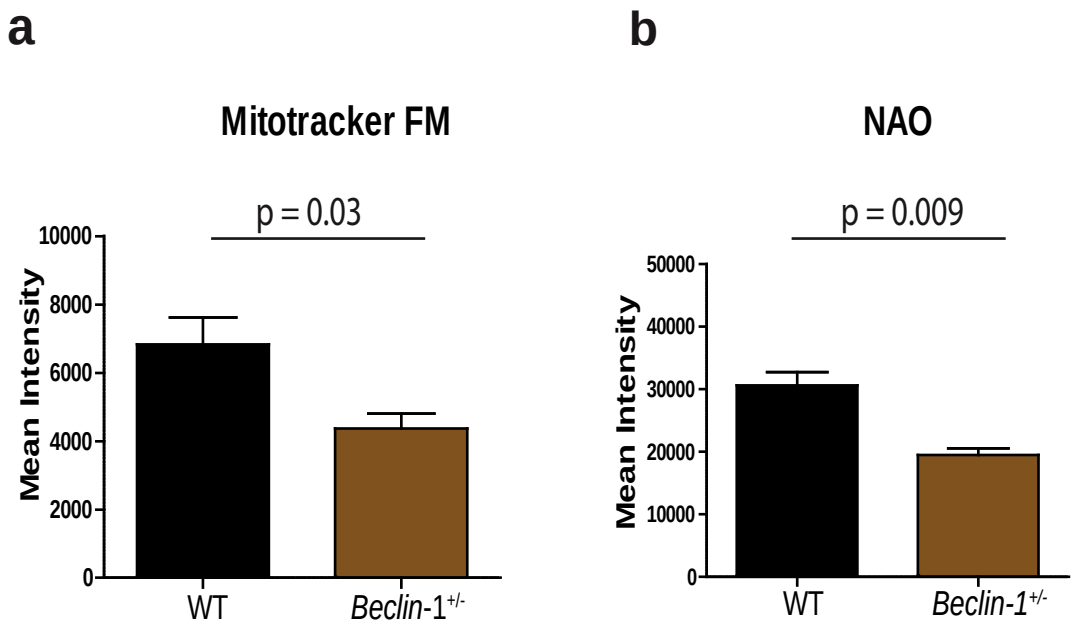
a
Mitotracker FM
p = 0.03
Mean Intensity
10000
8000
6000
4000
2000
0
WT
Beclin-1+/-
b
NAO
p = 0.009
Mean Intensity
50000
40000
30000
20000
10000
0
WT
Beclin-1+/-

**Figure S10**

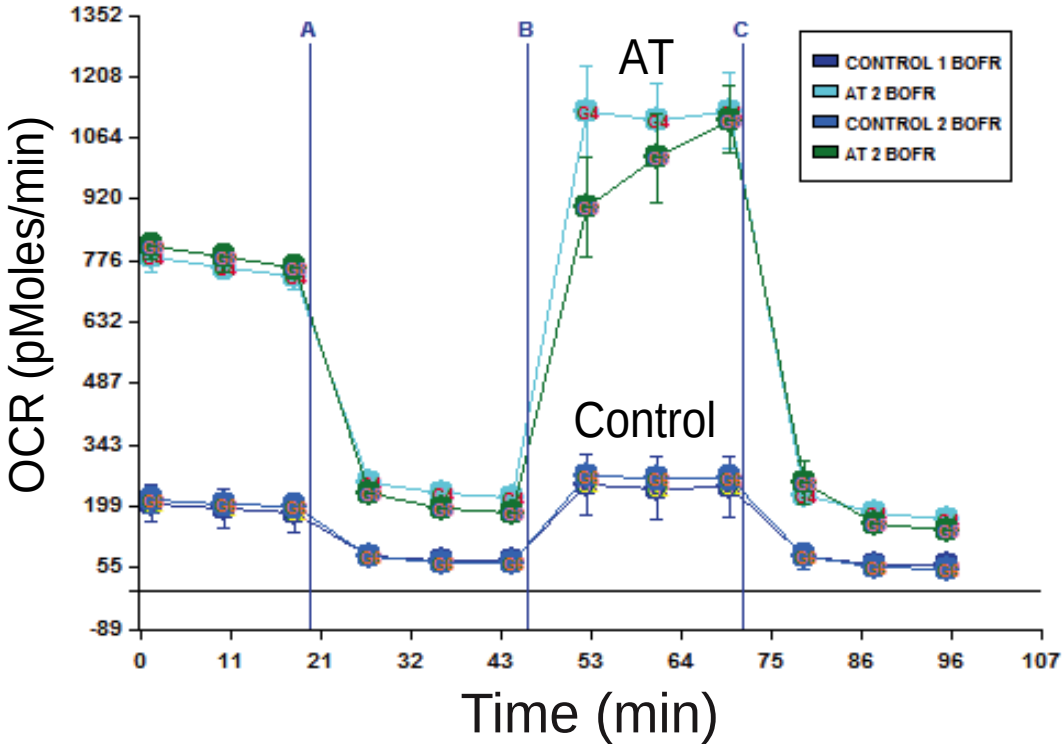
OCR (pMoles/min)
1352
1208
1064
920
776
632
487
343
199
55
-89
A
B
C
AT
Control
CONTROL 1 BOFR
AT 2 BOFR
CONTROL 2 BOFR
AT 2 BOFR
0
11
21
32
43
53
64
75
86
96
107
Time (min)

# Figure S11

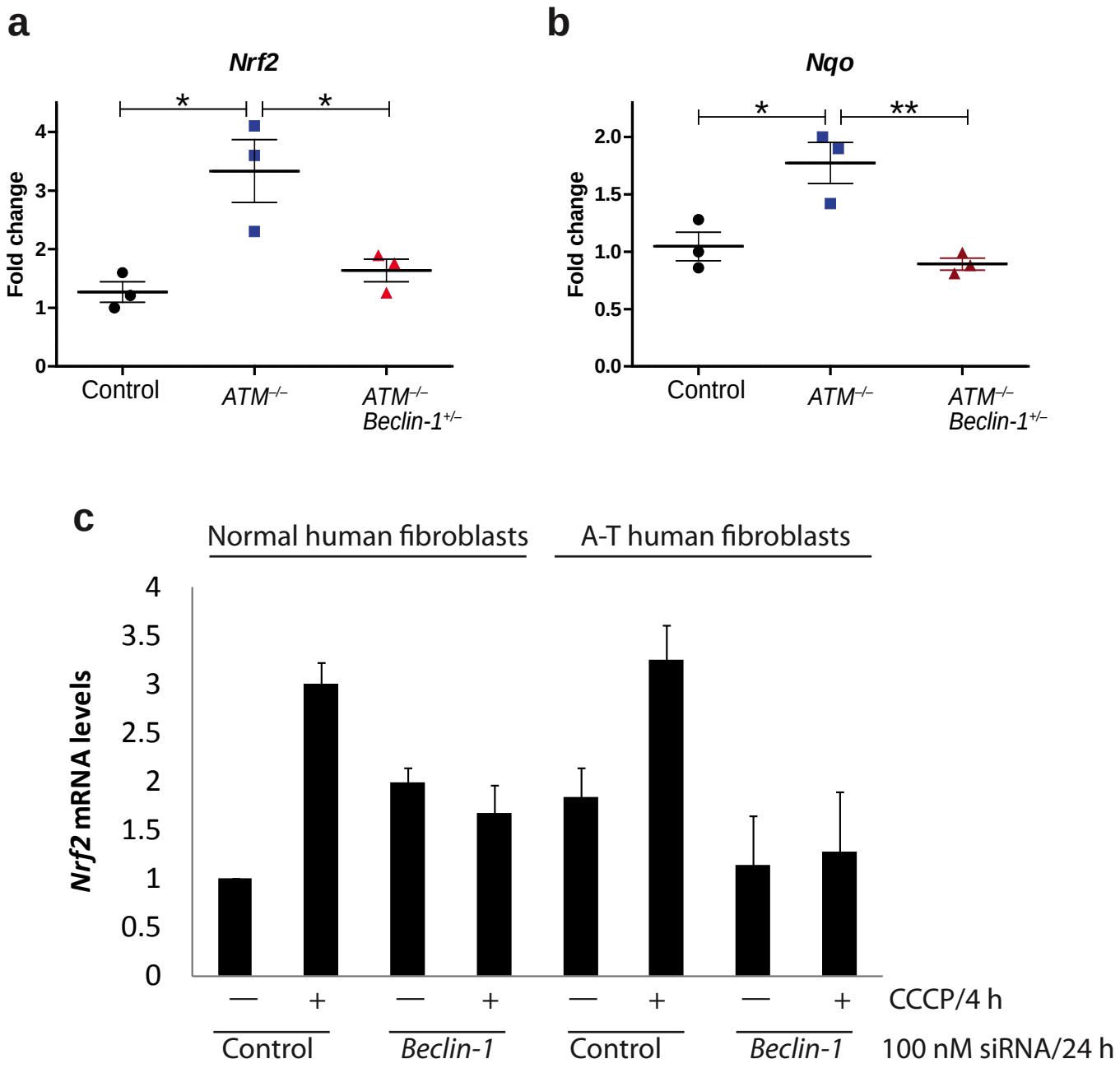
a
Nrf2
Fold change
0
1
2
3
4
*
*
Control
ATM-/-
ATM-/- Beclin-1+/-
b
Nqo
Fold change
0.0
0.5
1.0
1.5
2.0
*
**
Control
ATM-/-
ATM-/- Beclin-1+/-
c
Normal human fibroblasts
A-T human fibroblasts
Nrf2 mRNA levels
0
0.5
1
1.5
2
2.5
3
3.5
4
— + — + — + — +
CCCP/4 h
Control
Beclin-1
Control
Beclin-1
100 nM siRNA/24 h

# Figure S12

## B cells

### Mitotracker CMXRos

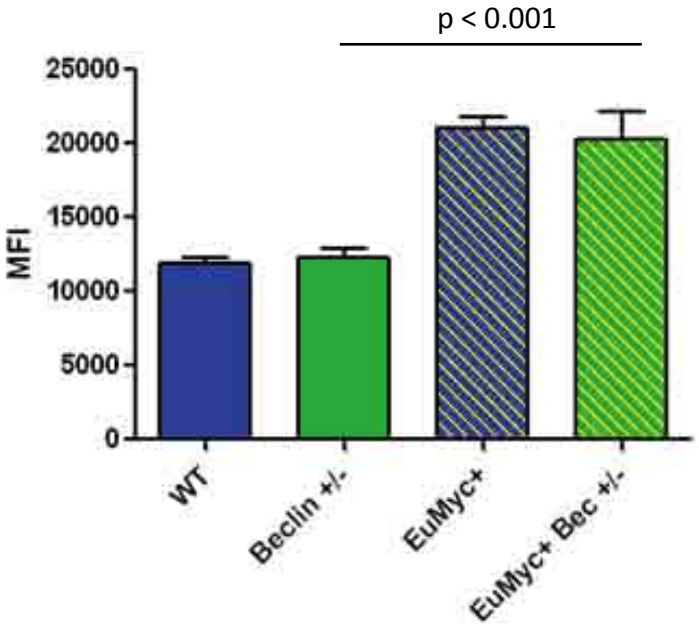

**Figure S13**

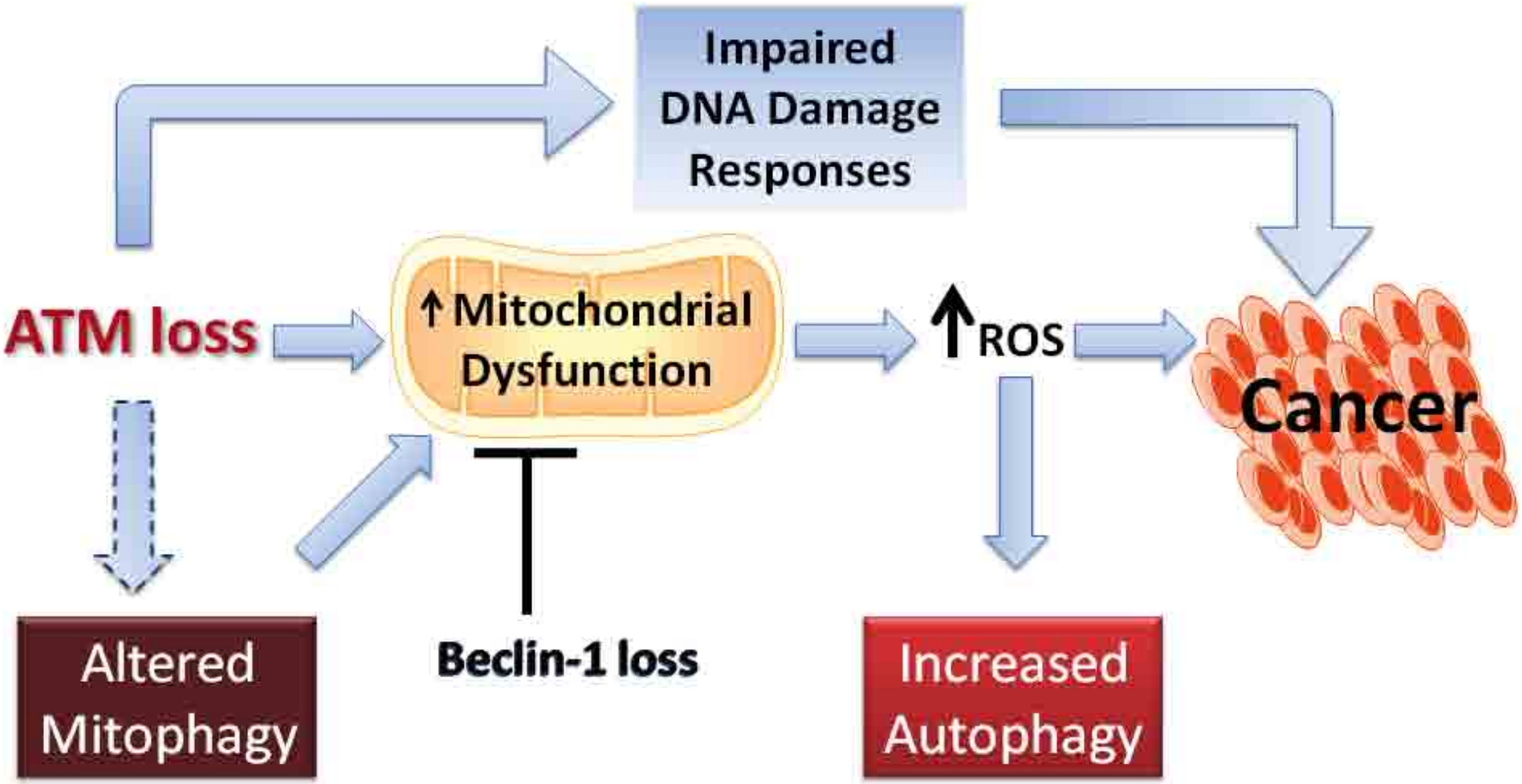
Impaired
DNA Damage
Responses
ATM loss
↑ Mitochondrial
Dysfunction
↑ ROS
Cancer
Altered
Mitophagy
Beclin-1 loss
Increased
Autophagy

# Figure S14

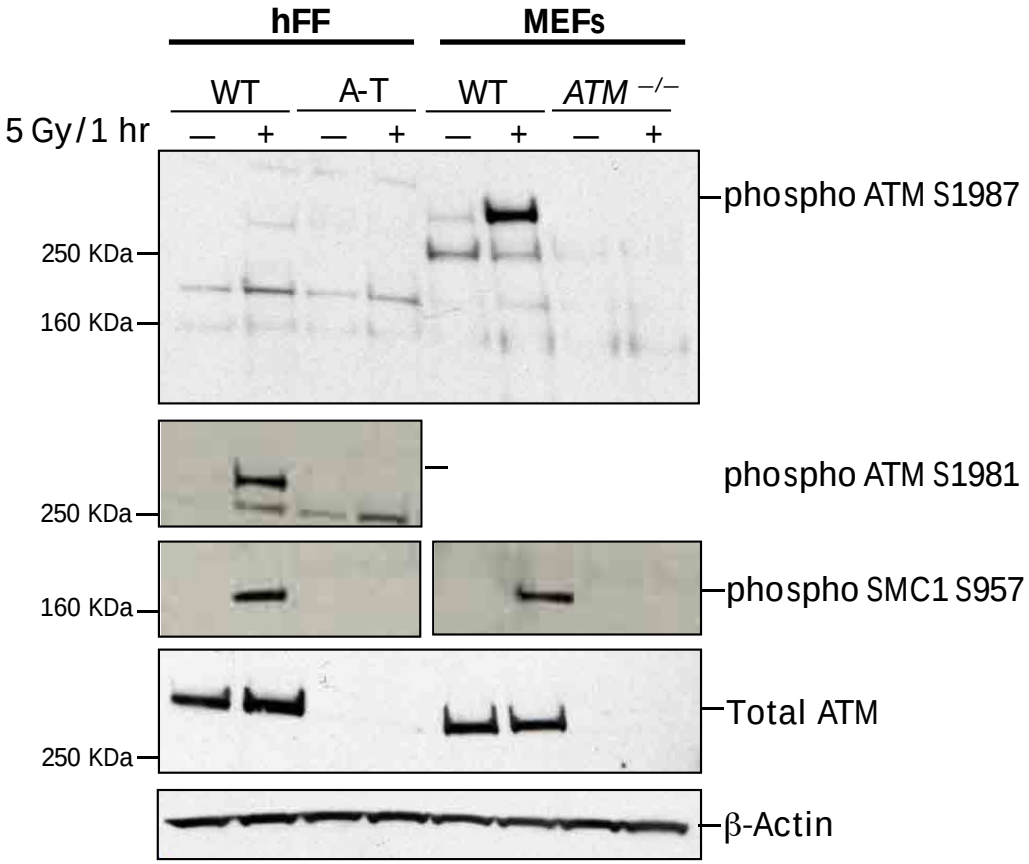
hFF
MEFs
WT
A-T
WT
ATM −/−
5 Gy/1 hr
— + — + — + — +
phospho ATM S1987
250 KDa
160 KDa
phospho ATM S1981
250 KDa
phospho SMC1 S957
160 KDa
Total ATM
250 KDa
β-Actin